UC Merced
UC Merced Previously Published Works

Title

Transcription factor complex AP-1 mediates inflammation initiated by Chlamydia pneumoniae infection.

Permalink

https://escholarship.org/uc/item/8rz3x3dp

Journal

Cellular microbiology, 15(5)

ISSN

1462-5814

Authors

Wang, Anyou
Al-Kuhlani, Mufadhal
Johnston, S Claiborne
et al.

Publication Date

2013-05-01

DOI

10.1111/cmi.12071

Peer reviewed

Transcription factor complex AP-1 mediates inflammation initiated by *Chlamydia pneumoniae* infection

Anyou Wang,[1][†] Mufadhal Al-Kuhlani,[2]
S. Claiborne Johnston,[3] David M. Ojcius,[2]
Joyce Chou[1] and Deborah Dean[1,4,5]*

[1]*Center for Immunobiology and Vaccine Development, Children's Hospital Oakland Research Institute, Oakland, CA 94609, USA.*

[2]*Health Sciences Research Institute and Molecular Cell Biology, University of California, Merced, CA 95340, USA.*

Departments of [3]*Neurology and*

[4]*Medicine, University of California School of Medicine, San Francisco, CA 94143, USA.*

[5]*Department of Bioengineering, University of California, Berkeley, CA 94720, USA.*

Summary

Chlamydia pneumoniae **is responsible for a high prevalence of respiratory infections worldwide and has been implicated in atherosclerosis. Inflammation is regulated by transcription factor (TF) networks. Yet, the core TF network triggered by chlamydiae remains largely unknown. Primary human coronary artery endothelial cells were mock-infected or infected with** ***C. pneumoniae*** **to generate human transcriptome data throughout the chlamydial developmental cycle. Using systems network analysis, the predominant TF network involved receptor, binding and adhesion and immune response complexes. Cells transfected with interfering RNA against activator protein-1 (AP-1) members FOS, FOSB, JUN and JUNB had significantly decreased expression and protein levels of inflammatory mediators interleukin (IL)6, IL8, CD38 and tumour necrosis factor compared with controls. These mediators have been shown to be associated with** ***C. pneumoniae*** **disease. Expression of AP-1 components was regulated by MAPK3K8, a MAPK pathway component. Additionally, knock-down of JUN and FOS showed significantly decreased expression of Toll-like receptor (TLR)3 during infection, implicating JUN and FOS in TLR3 regulation. TLR3 stimulation led to elevated IL8. These findings suggest that** ***C. pneumoniae*** **initiates signalling via TLR3 and MAPK that activate AP-1, a known immune activator in other bacteria not previously shown for chlamydiae, triggering inflammation linked to** ***C. pneumoniae*** **disease.**

Introduction

Inflammation is a natural biological response to stimuli such as microbial infection. Chronic inflammation, however, can lead to severe human diseases such as atherosclerosis and cancer (Karin *et al.*, 2006). The extent of inflammation is tightly controlled by transcription factors (TFs). For example, the NF-κB complex of TFs mediates inflammation involved in antimicrobial bioprocesses and disease pathogenesis (Pikarsky *et al.*, 2004). Yet, the key TFs that control inflammation initiated by a particular pathogen remain elusive.

Chlamydia pneumoniae is an obligate intracellular bacterial pathogen that is responsible for a high prevalence of upper and lower respiratory tract infections worldwide (Campbell and Kuo, 2004). *C. pneumoniae* has also been implicated in atherosclerosis based on compelling evidence from *in vitro* and animal studies in addition to data from human populations (Selzman *et al.*, 2003; Belland *et al.*, 2004; Campbell and Kuo, 2004). Some of the most persuasive evidence comes from the direct initiation or exacerbation of vascular lesions in rabbit and murine models in response to *C. pneumoniae* infection (Selzman *et al.*, 2003; Belland *et al.*, 2004; Campbell and Kuo, 2004).

Human hosts activate multiple TFs such as AP-1 and NF-κB that mediate inflammation (Dechend *et al.*, 1999; Miller *et al.*, 2000; Huang *et al.*, 2008). The NF-κB complex has been regarded as a major TF complex in the regulation of inflammation caused by *C. pneumoniae* infection (Dechend *et al.*, 1999). However, recent discoveries reveal that NF-κB is not necessary for the

stimulation of inflammation during *Chlamydia trachomatis* infection (Misaghi *et al.*, 2006; Le Negrate *et al.*, 2008). This organism actually stimulates the formation of a protein complex, ChlaDub1, to inhibit NF-κB activation (Misaghi *et al.*, 2006; Le Negrate *et al.*, 2008), suggesting that NF-κB may not be the most important complex controlling inflammation initiated by chlamydiae (Le Negrate *et al.*, 2008), although this has not yet been shown for *C. pneumoniae*. Nevertheless, with or without NF-κB, the human host activates a variety of inflammatory responses and releases various cytokines to cope with *C. pneumoniae* infection. For example, IL-8, which contains promoters for multiple TFs including binding sites for AP-1 and NF-κB, is released during *C. pneumoniae* infection of endothelial cells (Krull *et al.*, 2004) and is linked to inflammatory disease development at this site (Campbell and Kuo, 2004; Krull *et al.*, 2004). This suggests that at least one alternative TF complex other than NF-κB is activated in response to *C. pneumoniae*.

An obvious candidate is the AP-1 complex, a ubiquitous dimeric protein complex composed of Jun (e.g. JUN) and Fos (e.g. FOS) subfamilies (Curran and Franza, 1988). AP-1 is commonly activated during microbial infection with bacteria and viruses (Seo *et al.*, 2004; Xie *et al.*, 2005). In *in vitro* studies, *C. pneumoniae* infection of human vascular smooth muscle cells induced both NF-κB and AP-1 (Miller *et al.*, 2000). In the murine model, the product of the immediate early gene c-Fos (FOS), a subunit of AP-1, is activated in the heart during *C. pneumoniae* infection (Huang *et al.*, 2008).

Similar to NF-κB, AP-1 contains transcriptional regulator binding sites for most inflammatory mediators, and AP-1 can also bind promoters of inflammatory mediators independent of NF-κB during inflammation (Cho *et al.*, 2001; Balasubramanian *et al.*, 2003). Therefore, AP-1 independently mediates the release of inflammatory mediators such as IL8 (Yeo *et al.*, 2004). AP-1 also interacts with other TFs to modulate expression of inflammatory mediators during infection with pathogens such as Group B Streptococcus (Vallejo *et al.*, 2000). AP-1 functions vary depending on the combination of AP-1 complex components and conditions. The FOS and JUN complexes normally function as positive factors in regulating inflammation (Shaulian and Karin, 2002). However, the functional complexity of AP-1 remains largely elusive.

In the present study, we employed a systems biology network approach and identified AP-1 as the core complex modulating the fundamental processes of inflammation, including inflammatory signalling initiation, the signalling cascade and inflammatory mediator releases, in response to *C. pneumoniae* infection. The model predicted a role for TLR3 in initiating the inflammatory response, which was confirmed by infecting cells expressing different TLRs. Our results provide a unifying mechanism by which *C. pneumoniae* regulates inflammation.

Results

AP-1 members are the core components of a TF network Initiated by *C. pneumoniae* infection

To systematically decode a TF network involved in inflammation initiated by *C. pneumoniae* infection, we applied a protein-based network approach to analyse expression profiling altered by *C. pneumoniae* infection. We first assembled a protein interaction network by integrating the known protein-interaction databases as we previously published (Wang *et al.*, 2010). We then mapped the network with the transcriptome data that was significantly altered by *C. pneumoniae* infection in HCAEC, a primary cell line used as a model for studying arthrosclerosis and *C. pneumoniae* infection (Molestina *et al.*, 1998; Kaul and Wenman, 2001; Hogdahl *et al.*, 2008). HCAEC were infected with live *C. pneumoniae* at five time points, representing the developmental cycle of the organism. The time points corresponded to bacterial attachment (5 min post infection), entry (25 min), initial transformation into metabolically active reticulate bodies and replication (2 h), metabolism and replication (24 h) and transformation into infectious particles for release and infection of adjacent cells (60 h). The transcription alterations during infection with living bacteria were compared with those from UV-treated *C. pneumoniae* and mock-infected HCAEC.

The TFs with significantly altered expression during *C. pneumoniae* infection were mapped to their corresponding proteins in the above network to integrate the gene expression profiling and network database as we previously described (Wang *et al.*, 2010). The overlaid network became a dynamic TF network activated by *C. pneumoniae* infection (Figs 1A and 2).

To identify the key TFs in the infection model, we searched for the hubs and bottlenecks (Yu *et al.*, 2007) in the TF network as we previously described (Wang *et al.*, 2010). We systematically *in silico* knocked out each TF and examined their contribution to network connectivity – the distance between a node and every other node in the transmission range – calculated as the average number of neighbours (i.e. average distance). The TFs that contributed most to the connectivity of the network at 5 min were FOS (v-fos FBJ murine osteosarcoma viral oncogene homologue), EGR1 (early growth response) and MAP3K8 (mitogen-activated protein kinase kinase kinase 8) (Fig. 1B, grey bars). In addition, we further calculated the contribution of a single TF to the network diameter – the average of the shortest path length, which essentially characterized the network's interconnectivity (Wang *et al.*, 2010). The longer the diameter, the less interconnectivity

there is in the network. Knocking out a hub (highly con-nected protein) would increase the diameter because of the loss of short paths in a network, whereas knocking out a bottleneck (node with many short paths going through them, analogous to key bridges that link subnetworks to a whole map network) (Yu *et al*., 2007), would decrease the diameter because the network would be broken down and the long path that normally links subnetworks would be lost. Knocking out FOS dramatically increased the network diameter (Fig. 1B, black bar), indicating that it is a hub in this network. However, knocking out SFPQ (splic-ing factor proline/glutamine rich – polypyrimidine tract binding protein associated) remarkably decreased the network diameter (Fig. 1B, black bar), and SFPQ also notably contributed to network connectivity (Fig. 1B, grey bar), suggesting that SFPQ is a bottleneck in this network. Deleting hub FOS (Fig. 2, green arrow) caused a huge loss in network connectivity. This suggested that the FOS hub and SFPQ bottleneck (Fig. 2, pink arrow) are critical co-ordinators in the network activated by *C. pneumoniae* at 5 min.

Similarly, the top 10 nodes that contributed to the network diameter for the rest of the time points are sum-marized in Fig. 1C. The top two hubs at 25 min were identified as FOS and AP-C (Activated Protein C), FOS and JUNB at 2 h, FOS and STAT1 at 24 h, and JUN and STAT1 at 60 h (Fig. 1C). Clearly, from the frequency of each TF in the entire profiling, FOS and JUN predomi-nated in these dynamic networks, indicating that the AP-1 complex is likely the core component of the inflammatory network initiated by *C. pneumoniae*.

The microarray data have been deposited in GEO. The accession number is GSE27008 (http://www.ncbi.nlm.nih.gov/geo/query/acc.cgi?token=vduzheioawcigtm&acc=GSE27008).

AP-1 regulatory network

After deducing that the AP-1 complex is likely the core component of the inflammatory network stimulated by *C. pneumoniae*, we searched for additional members of the AP-1 regulatory network. We mapped the known protein–protein interactions with inflammatory genes that are associated with the AP-1 complex and that were significantly altered after *C. pneumoniae* infection of HCAEC (Fig. 3A). Special attention was paid to genes that have putative AP-1-binding motifs predicted from the motif-binding matrix (http://xerad.systemsbiology.net/MotifMogulServer/) with constraint criteria as shown in Fig. 4. Most of these inflammatory genes exhibit more than two putative AP-1 binding sites located within 3000 base pairs upstream of the transcriptional start sites. Examples are shown in Figs 3B and 4. The mapped network containing these AP-1 targets became an AP-1

regulatory network that was further classified into func-tional protein complexes based on gene functions and cellular locations in the gene ontology database (Fig. 3A) (http://www.geneontology.org). This network, then, con-tained a number of primary complexes central to inflam-mation, including receptor (yellow), binding and adhesion (green) and immune response (red) complexes (Fig. 3A). These protein interactions have largely been known to be dynamically activated by the AP-1 complex. For example, the features of inflammation induced by *C. pneumoniae* infections in *in vitro* studies and murine models, such as inflammatory mediators IL6, IL8, CD38 and TNFα (Selzman *et al*., 2003; Belland *et al*., 2004; Campbell and Kuo, 2004) and key signalling kinases like MAP3K8, were among the factors included in these complexes.

AP-1 complex mediates expressions of inflammatory mediators

To confirm the role of AP-1 in inflammation as predicted above, we experimentally examined the effect of AP-1 on the expression of inflammatory factors IL6, IL8, TNFα and CD38 during *C. pneumoniae* infection of HEp-2 and human peripheral blood monocytic leukaemia (THP-1; ATCC TIB-202) cells. siRNA designed against AP-1 members FOS, FOSB, JUN and JUNB (Table S1) were used to knock down expression of each in addition to the combination knock-down of FOS and JUN. The knock-down efficiency was determined by measuring gene expression alteration of IL6, IL8, TNFα and CD38 by qRT-PCR (Table S2).

siRNA treatment successfully knocked down at least 75% of the gene expression for AP-1 components FOS, FOSB, JUN and JUNB (Fig. 5A). Knock-down of AP-1 significantly reduced expression of almost all examined inflammatory factors (Fig. 5B–E) in both HEp-2 and THP-1 cells except for IL6 in THP-1 cells with FOS$^-$ (Fig. 5D). Notably, the combined knock-down of AP-1 components produced, in general, a greater reduction of inflammatory gene expression than any single AP-1 member knock-down (Fig. 5B–E). For example, IL6 expression was not significantly altered under single FOS knock-down in THP-1 cells, but was dramatically repressed under the combination knock-down of FOS$^-$JUN$^-$. These findings suggested that AP-1 dimers are crucial TFs for inflammatory mediator release during *C. pneumoniae* infection.

The expression levels of selected inflammatory genes were also verified at the protein level using a Luminex multiplex protein quantitative assay (Fig. 5F). In general, results measured at the protein and mRNA level were consistent. Both FOS$^-$ and JUN$^-$ resulted in significantly lower protein levels of IL8 and TNFα compared with the
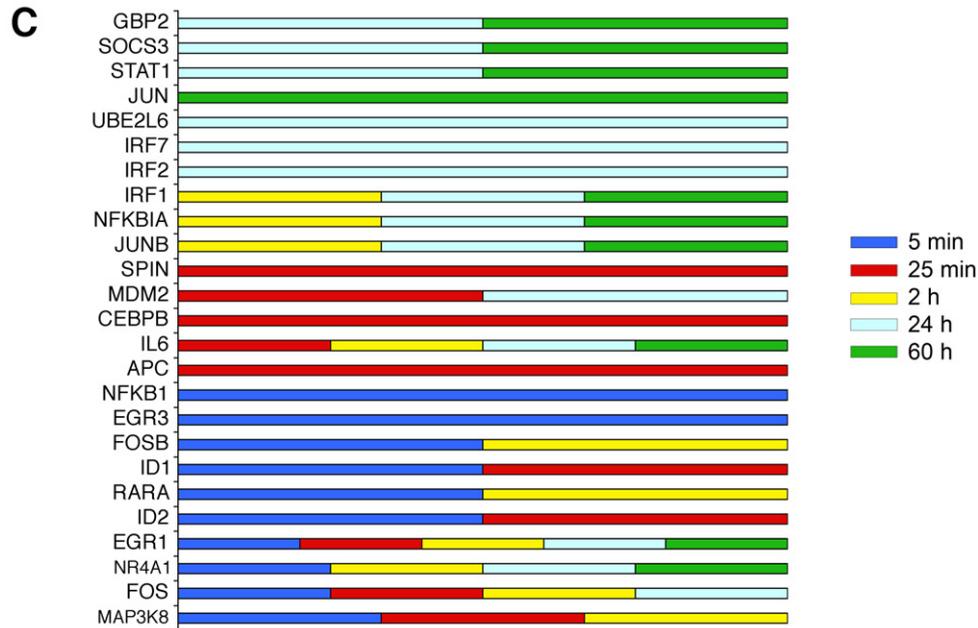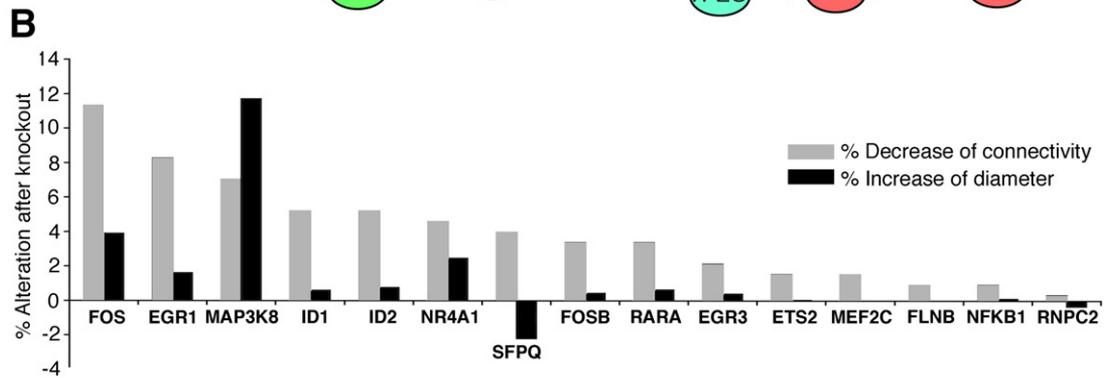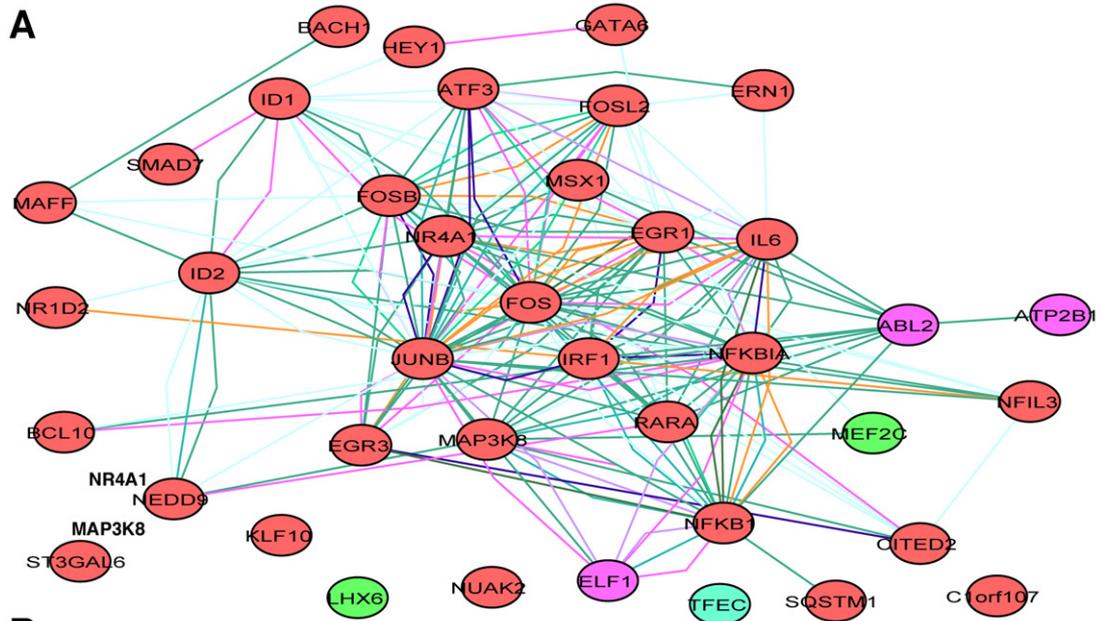
Fig. 1. AP-1 components dominate the transcription factor (TF) network initiated by *C. pneumoniae* infection of HCAEC.
A. AP-1 components, FOS, FOSB and JUNB dominate the TF network initiated by *C. pneumoniae* infection. The TF network was derived from a genome-wide protein interaction network overlapped with transcriptome data from this study (see *Experimental procedures*). Nodes and edges donate proteins and interactions respectively. The colour of the node represents the gene expression level: Red for upregulation, green for downregulation and violet for equivocal at 5 min.
B. The contribution of TFs to network connectivity and to the diameter of the network activated at 5 min post infection. TFs were systematically knocked out *in silico,* and the alterations in network connectivity (measured as average number of neighbours) and network diameter (measured as average shortest path length) were calculated (see *Experimental procedures*). The top TFs that contributed most to the network are shown. FOS and MAP3K8 contributed the most to both connectivity and diameter, respectively, suggesting that AP-1 dominates the TF network for *C. pneumoniae.*
C. Summary of the top 10 TFs from our transcriptome data at each time point that contributed the most to the diameter of the network activated at 5 min, 25 min, 2 h, 24 h and 60 h. From top to bottom, GBP2, SOCS3, STAT1, JUN, UBE2L6, IRF7 and IRF2 predominated in late infection (24 h and 60 h), while IRF1, NFKIA and JUNB were featured at 2 h, 24 h and 60 h. SPIN, MDM2, CEBPB and APC predominated at 25 min. EGR1, NR4A1, IL6 and FOS were primarily activated from 5 min to 24 h or to 60 h.

control. Together, our data suggest that AP-1 is a key TF complex regulating inflammation initiated by *C. pneumoniae* infection.

AP-1 complex mediates inflammatory signalling via TLR3 and MAP3K8

We next explored the mechanisms for AP-1 regulation of inflammation by examining the key inflammatory pathway regulated by AP-1 during *C. pneumoniae* infection. Inflammatory signalling is initiated by pattern recognition receptors (PRR), which then precipitate a signalling cascade via protein kinases. To identify crucial genes primarily involved in inflammation regulated by AP-1, we systematically screened genes with the highest correlation with AP-1 based on both the AP-1 target network (Fig. 3) and the mathematical model analysis of coexpression profiling. Gene expression alterations of all components of the AP-1 regulatory network (Fig. 3A) were measured by qRT-PCR for both overexpression of AP-1 (wild-type) and knock-down of AP-1 (FOS⁻, JUN⁻ and combination FOS⁻JUN⁻) via siRNA during *C. pneumoniae* infection of HCAECs. A standard stepwise regression model was used to select genes with the largest partial correlation with AP-1. The results showed that AP-1 strongly associates with TLR3 and MAP3K8. Based on gene ontology (Fig. 3A), TLR3 appeared to be targeted by AP-1, while MAP3K8 appeared to be the key kinase for signalling transduction. We found that JUN and FOS knock-down significantly inhibited TLR3 expression (Fig. 6A) but not TLR4. TLR2 expression was similarly inhibited. By plotting the dynamic gene expression pattern of AP-1 components and MAP3K8 for 5 min, 25 min, 2 h, 24 h and 60 h, we found similar expression patterns between AP-1 complex TFs and MAP3K8 in HCAECs (Fig. 6B), which is consistent with the general regulatory pathway induced by pathogens as previously reported by Nijhara *et al.* (2001). Together, these data demonstrate that the AP-1 complex mediates inflammatory signalling via TLR3 and MAP3K8.

TLR3 regulates activation of NF-κB and expression of the chemokine IL8

TLR2 was previously shown to stimulate the innate immune response during infection by *Chlamydia muridarum* and *C. pneumoniae*, while TLR4 is thought to have no effect (Prebeck *et al.*, 2001; Darville *et al.*, 2003; Naiki *et al.*, 2005; Cao *et al.*, 2007). A role for TLR3 has been reported for infection of an oviduct cell line by the murine pathogen, *C. muridarum* (Derbigny *et al.*, 2005; 2007; 2010) but never in animal studies. TLR3 effects on infection by the human pathogens, *C. trachomatis* or *C. pneumoniae*, have never been studied. Given our unexpected finding that the AP-1 complex regulates signalling via TLR3 during *C. pneumoniae* infection, we screened the TLRs likely to be involved in the response to *C. pneumoniae* using HEK293 cells that are stably transfected with control vector or human TLR2, TLR3 or TLR4. The cells, including control cells, stably coexpress an NF-κB-inducible SEAP (secreted embryonic alkaline phosphatase) reporter gene whose enzymatic activity can be conveniently and quantitatively monitored through a colorimetric assay.

As expected, HEK cells expressing NF-κB-induced reporter gene but not TLR (HEK-Null1) did not show NF-κB activation in response to stimulation with ligands for TLR2 (Pam3), TLR4 (LPS) or TLR3 (Pam3), or infection with C. *pneumoniae* (Fig. 7A). However, *C. pneumoniae* infection or Pam3-stimulation induced strong NF-κB activation in HEK-TLR2 cells, in agreement with previous reports. *C. pneumoniae* infection had no effect in HEK-TLR4 cells, although the positive control, LPS, stimulated NF-κB activation in these cells. *C. pneumoniae* infection had no effect at low multiplicity of infection (moi) in TLR3-expressing cells, but activated NF-κB at significant levels at an moi of 10 or 40. Even at the highest moi, there was no NF-κB in the HEK-Null1 cells.

The same cells were also used to measure IL8 gene expression during *C. pneumoniae* infection (Fig. 7B). IL8 expression in HEK-TLR3 cells was observed even at low moi of infection. Much higher levels of expression were
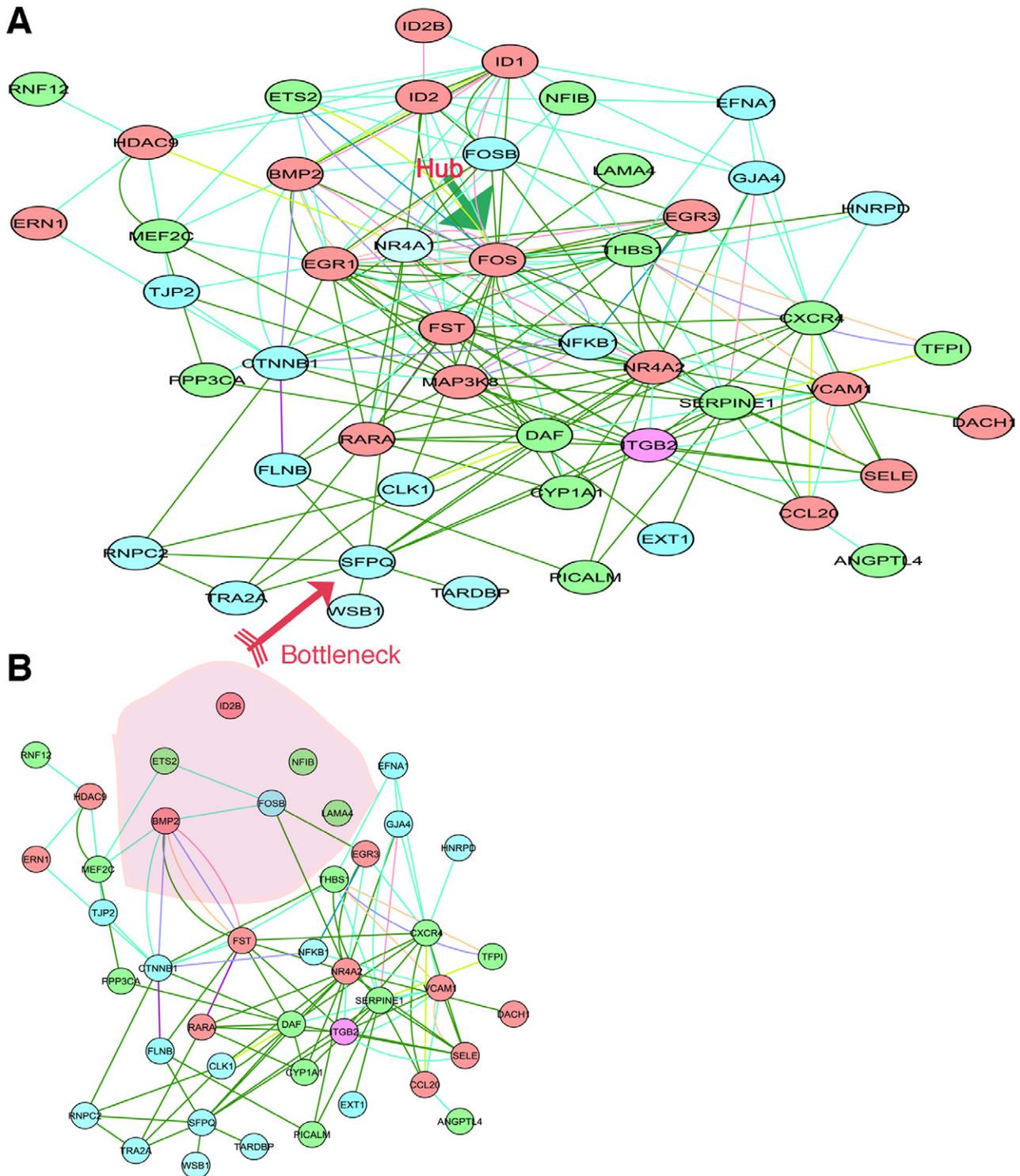
Fig. 2. *In silico* knockout of hubs and bottlenecks in the TF network.
A. Hubs and bottleneck and their neighbours for the wild-type network activated at 5 min. The green arrow highlights a hub (FOS). The pink arrow highlights a bottleneck (SFPQ).
B. The network was locally disconnected after the combination of knocking out the first five genes, FOS, EGR1, MAP3K8, ID1 and ID2, compared with the wild-type network shown in (A).

A

B

-2107 CTGAATCAG -2099   -623 ATTACTCAG -615   -126 CTGAGTCAT -118

-2500   -2000   -1500   -1000   -500   +1
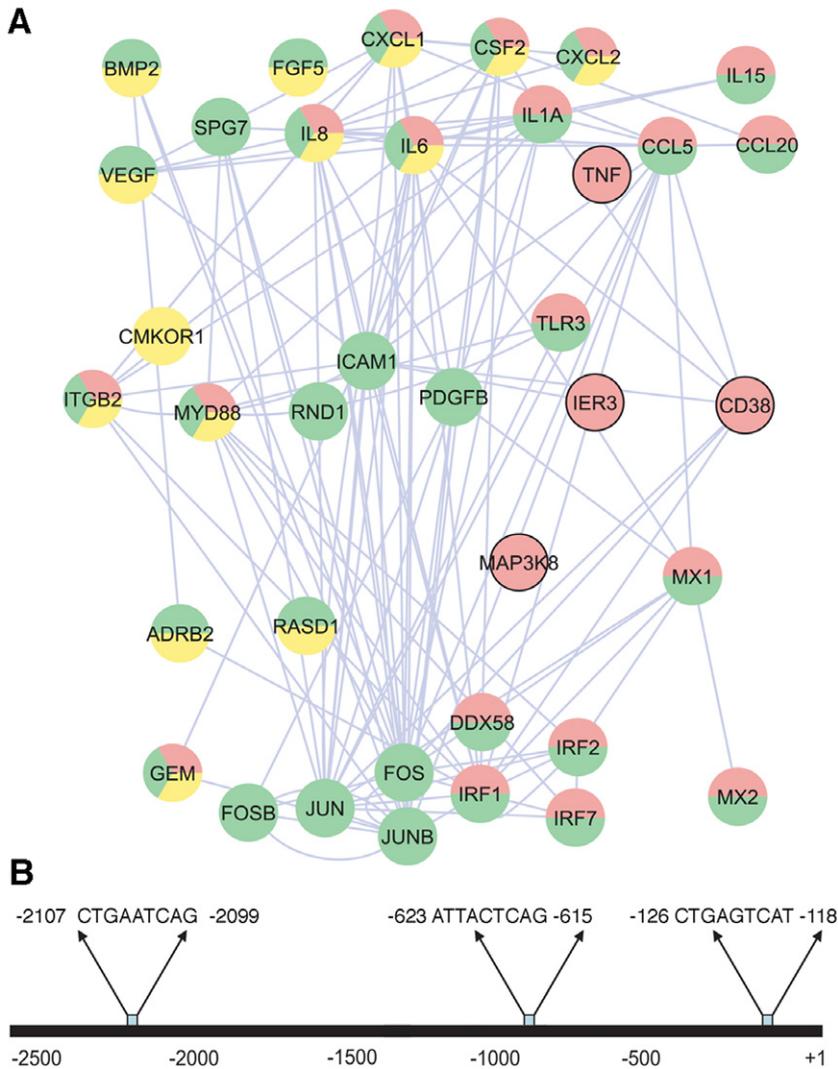
Fig. 3. AP-1 target gene predictions using the protein–protein interaction network and promoter sequence analysis.
A. Predicting AP-1-associated genes using the protein interaction network. The genes were determined from the network assembled from known transcription factor protein–protein interactions and transcriptome data as described in *Experimental procedures*. This network was organized by the gene ontology database, in which gene functions and localizations were included. AP-1 (nucleus) is predicted to interact with a number of major functional modules, including those for receptor complexes (yellow), immune response (red) and binding and adhesion (green).
B. Computational analysis of AP-1 binding sites for inflammatory mediators. These AP-1 binding sites were identified by scanning the 5′ upstream promoter regions of each gene with MotifMogul. For illustration, only the one for IL8 is shown; the rest are shown in Fig. 4.

found in HEK-TLR2 cells, also consistent with previous studies, although TLR3-dependent IL8 production during chlamydial infection has not been reported until now. *C. pneumoniae* infection, even at moi = 40, had no effect on IL8 expression in HEK cells in the absence of TLR.

Discussion

Inflammation is fundamentally modulated by TFs. However, the challenge has been to identify the critical TFs that regulate inflammation, because a complex network is usually activated during pathogenic infections. The NF-κB complex, a well-characterized TF complex, has been considered key in regulating inflammatory mediators (e.g. IL6 and IL8) during chlamydial infections (Gencay *et al.*, 2003; Buchholz and Stephens, 2006). However, recent studies argue against this (Le Negrate *et al.*, 2008). Significantly, chlamydial infection has been

reported to interfere with NF-κB signalling (Lad *et al.*, 2007; Le Negrate *et al.*, 2008; Betts *et al.*, 2009; Wolf *et al.*, 2009).

In the present study, we employed a systems biology approach and found that AP-1 contributes to the major structure of the TF network initiated by *C. pneumoniae* infection (Fig. 1) and regulates many inflammatory mediators (Fig. 3). RNAi knock-down of single components of AP-1 or the AP-1 dimer combination significantly reduced the expression of inflammatory mediators, such as IL6, IL8, CD38 and TNFα, at both the mRNA and protein level (Fig. 5), although the latter levels were not as low as might be expected given the corresponding gene knock-down. The inflammatory mediator IL8 has been reported to be regulated by NF-κB, but IL8 release also occurs through the MAPK pathway independently of the NF-κB complex during *C. trachomatis* infection (Lad *et al.*, 2007). Here, we revealed that IL8 is primarily regulated by AP-1. Our
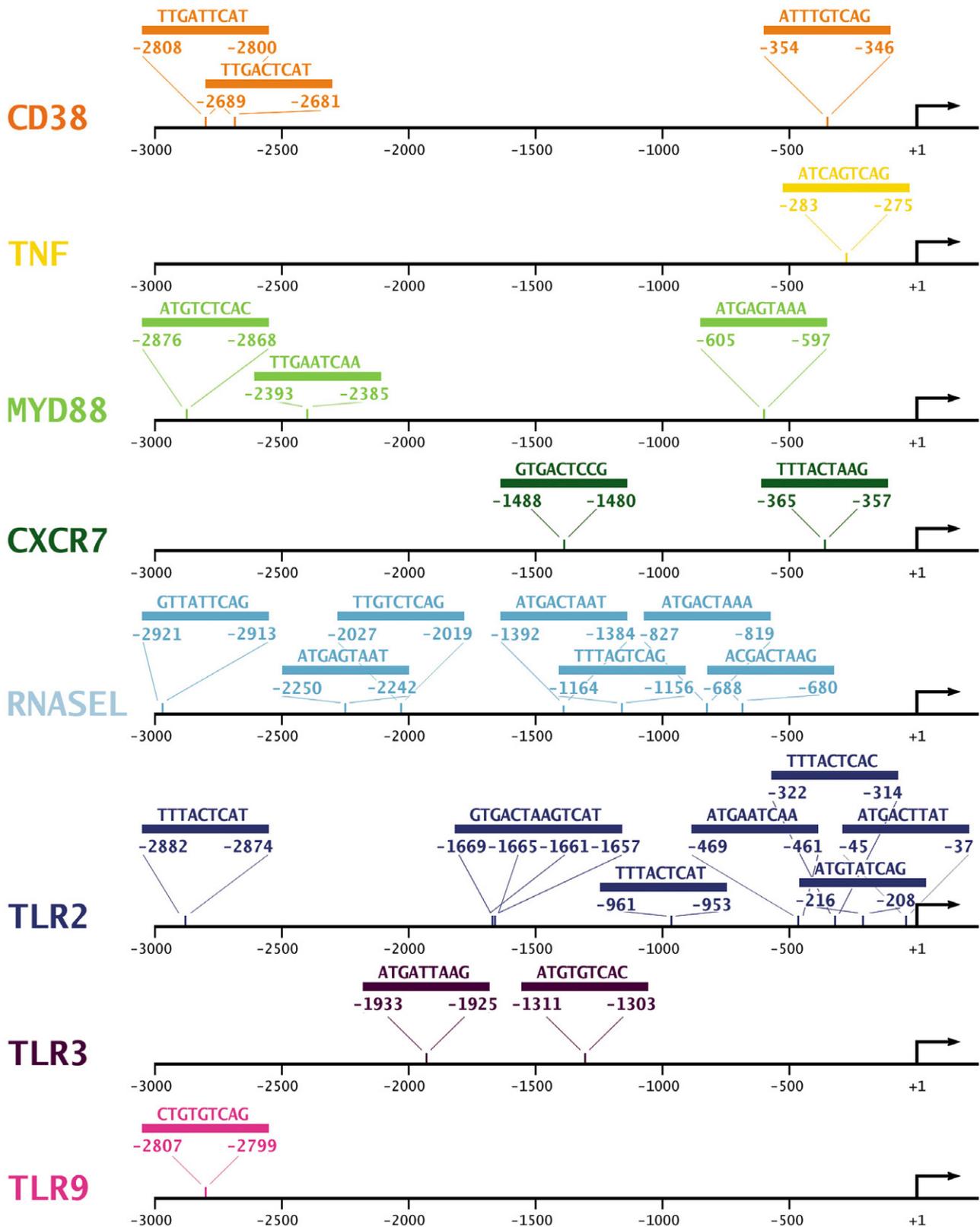
Fig. 4. AP-1 binding sites for inflammatory mediators predicted by MotifMogul. MotifMogul was used to predict AP-1 binding sites for inflammatory mediators as described in detail in *Experimental procedures*.
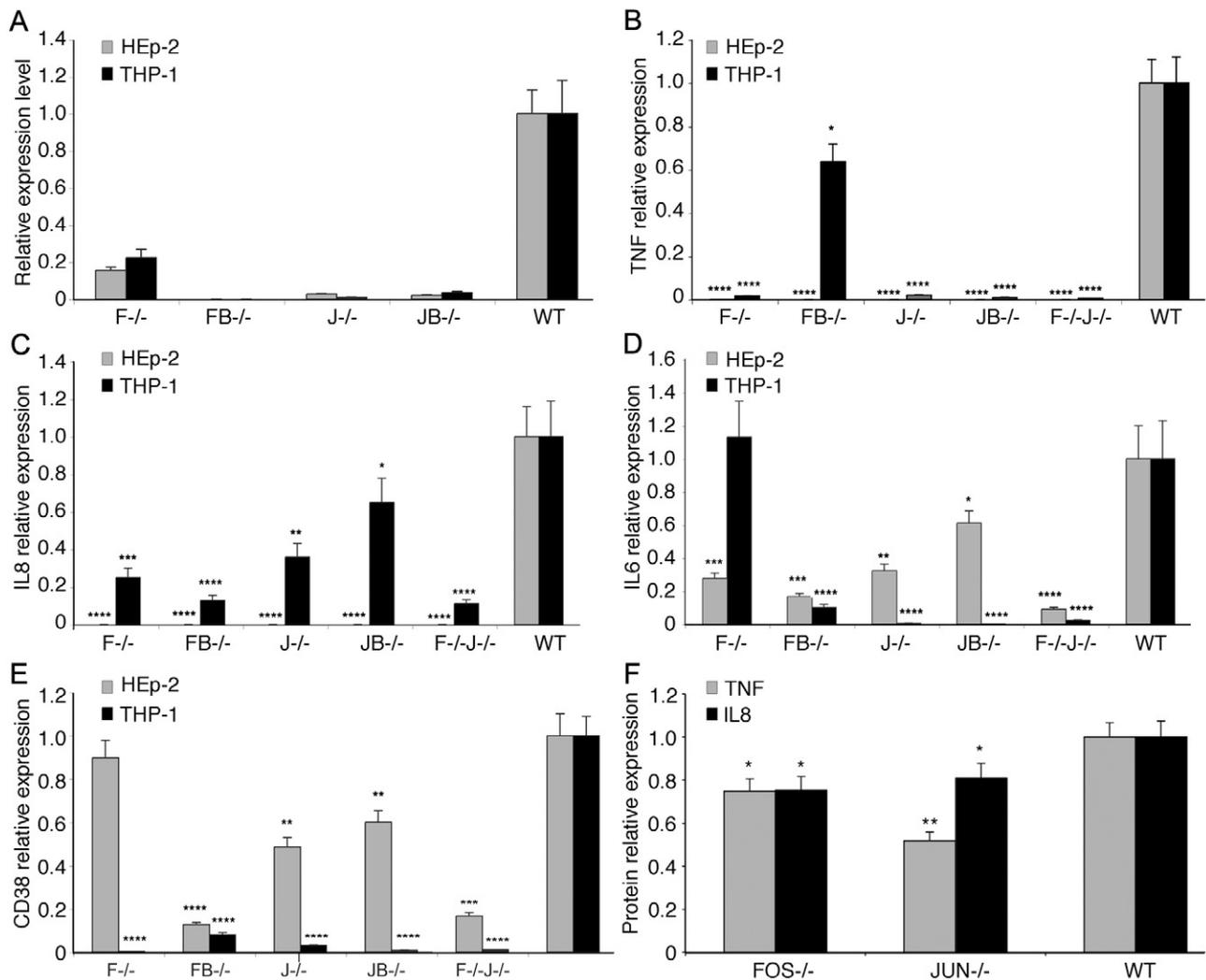
Fig. 5. AP-1 regulates gene expression of inflammatory mediators in *C. pneumoniae* infected HEp-2 and THP-1 cells.
A. AP-1 components FOS, FOSB, JUN and JUNB were knocked down by siRNA. The knock-down efficiency was determined by measuring gene expression alteration by qRT-PCR after siRNA knock-down of each AP-1 member (FOS, F–/–; FOSB, FB–/–; JUN, J–/–; JUNB, J–/–; FOS and JUN, F–/–J–/–) in *C. pneumoniae* infected HEp-2 and THP-1 cells. At least 75% of the gene expression of AP-1 members was knocked down when compared with the scrambled siRNA control.
B–E. Knock-down of AP-1 members FOS and JUN during *C. pneumoniae* infection significantly decreased key pro-inflammatory mediators TNF, IL8, IL6 and CD38, but not IL6, measured by qRT-PCR in both HEp-2 and THP-1 cells compared with wild-type (WT).
F. Knock-down of AP-1 components JUN and FOS downregulate inflammatory factors TNF and IL8 compared with WT measured during infection.
*$P < 0.045$, **$P < 0.01$, ***$P < 0.001$ and ****$P < 0.0005$.

findings suggest that AP-1 is a key TF complex that regulates the inflammatory network activated by *C. pneumoniae* infection.

AP-1 is a ubiquitous dimeric protein complex composed of different Jun (c-Jun, JunB and JunD) and Fos (c-Fos, Fra-1, Fra-2 and FosB) subfamilies (Curran and Franza, 1988) and commonly activated during microbial infection with bacteria and viruses (Seo *et al.*, 2004; Xie *et al.*, 2005). AP-1 complexes normally function as positive factors in regulating inflammation and the cell cycle. Yet, different combinations of AP-1 members express differen-

tial biological effects. While JUN, FOS and FOSB are often positively associated with inflammation, cell growth, cellular transformation, tumour formation and tumour progression, JUNB performs a negative regulatory role in mediating cell proliferation (Shaulian and Karin, 2002). AP-1 mediates the release of inflammatory mediators such as IL8 (Yeo *et al.*, 2004) and regulates angiogenesis caused by pathogen infection as in the case of herpesvirus infection (Ye *et al.*, 2007). AP-1 also interacts with other TFs to cope with pathogen development (Ravichandran *et al.*, 2006) and modulates expression
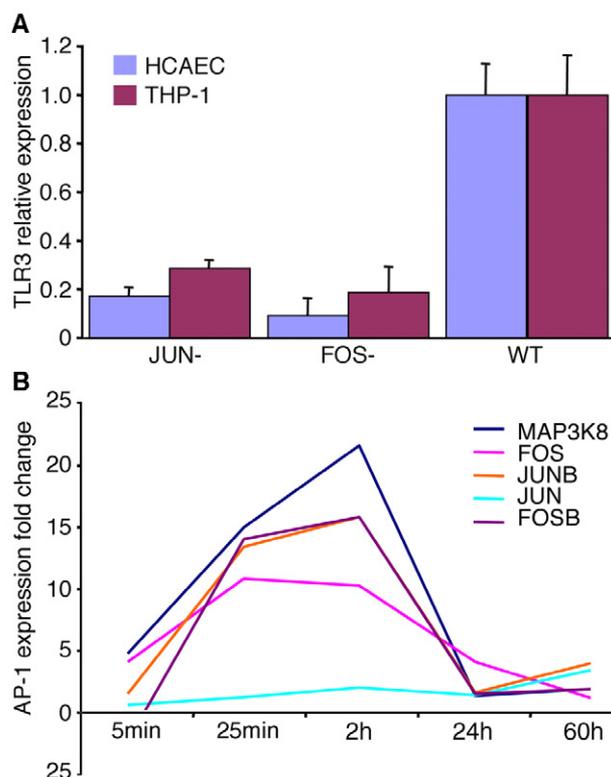
Fig. 6. AP-1 complex mediates inflammatory signalling via TLR3 and MAP3K8.
A. JUN and FOS knock-down by siRNA dramatically alters gene expression of TLR3 in *C. pneumoniae* infected HCAEC and THP-1 cells as measured by qRT-PCR.
B. Expression of AP-1 components correlates with MAPK signalling pathway during *C. pneumoniae* infection of HCAEC measured by both microarray and qRT-PCR.

of inflammatory mediators during infection with pathogens such as Group B Streptococcus (Vallejo *et al.*, 2000). This suggests that the biological functions of AP-1 are complex and that much of its functional complexity remains to be elucidated.

The function of AP-1 is known to vary depending on cell type (Chinenov and Kerppola, 2001; Eferl and Wagner, 2003). We used three different cell types to examine the AP-1 function during *C. pneumoniae* infection and surprisingly, found that inflammatory mediators, IL6, IL8, CD38 and IFN, were primarily regulated by most of the AP-1 members examined here. In fact, other inflammatory mediators predicted in Fig. 3A were also regulated by at least one AP-1 member (either FOS or JUN) for a given cell line. This suggests that AP-1 likely regulates inflammation stimulated by *C. pneumoniae* infection. Our results nicely parallel the recent observations showing that AP-1 serves as a crucial modulator in regulating inflammation initiated by other pathogens such as Group B streptococcus, Herpes simplex virus 1 and *Helicobacter pylori* (Zachos *et al.*, 1999; Vallejo *et al.*, 2000; Wu *et al.*, 2006).

The underlying molecular mechanism(s) whereby AP-1 mediates inflammation during infections remains largely unknown. Here, our data revealed that AP-1 is activated primarily from TLR3 and MAP3K8 signalling pathways during *C. pneumoniae* infection. TLR3 is a host PRR that recognizes dsRNA derived from many different viral pathogens (Takeuchi and Akira, 2009). The interaction of dsRNA with TLR3 and its ectodomain results in dimer formation and recruitment of TIR-domain-containing adapter-inducing interferon-β (TRIF) that initiates signalling pathways and ultimately downstream TF activation, including AP-1 (Botos *et al.*, 2009). While dsRNA is commonly produced by viral replication and is not known to be associated with chlamydiae, we speculate that it is possible that the organism generates a unique molecular ligand that is recognized by TLR3. In a murine oviduct cell line that was infected with *C. muridarum*, TLR3 was expressed in infected cells and served as a trigger for IFNβ production (Derbigny *et al.*, 2005), which was subsequently found to be dependent on interferon regulatory factor 3 (IRF3) and TRIF (Derbigny *et al.*, 2007). Recently, the IFNβ response was shown to be dependent on TLR3 in the same cell line (Derbigny *et al.*, 2010). In another study. *C. pneumoniae* induced foam cell formation was influenced by TLR2 and TLR4 but not TLR3 (Chen *et al.*, 2008). Our data revealed that TLR3 as well as interferon regulatory factors were activated during *C. pneumoniae* infection (Fig. 3) and regulated by JUN and FOS (Fig. 6). AP-1 may regulate inflammation via regulating TLR3, which appears to be one key receptor initiating inflammatory signalling triggered by *C. pneumoniae* infection, although signalling initiated by TLR3 can cascade via various pathways (Vercammen *et al.*, 2008).

In addition, our data showed that MAP3K8 is a key enzyme regulating AP-1 signalling during *C. pneumoniae* infection (Figs 2 and 4), which is consistent with previous reports showing that AP-1 is regulated by the MAPK pathway (Chinenov and Kerppola, 2001; Eferl and Wagner, 2003). Previous studies demonstrated that release of inflammatory mediators such as IL8 are dependent on the MAP pathway independent of NF-κB (Cho *et al.*, 2001; Balasubramanian *et al.*, 2003). We found that IL8 release was dependent on AP-1. Thus, our findings suggest a model wherein *C. pneumoniae* initiates inflammatory signalling via TLR3 and the MAPK pathway, which in turn activates AP-1, triggering inflammatory mediator and chemokine release that are linked to chlamydial disease (Darville *et al.*, 2003; Buchholz and Stephens, 2006; Sessa *et al.*, 2009).

The functions of different AP-1 components could vary considerably, as inducers or inhibitors depending on specific conditions. There are many pathways that can transmit the signalling, once initiated (Fig. 3). Our data showed that the FOS and JUN complex serves as a
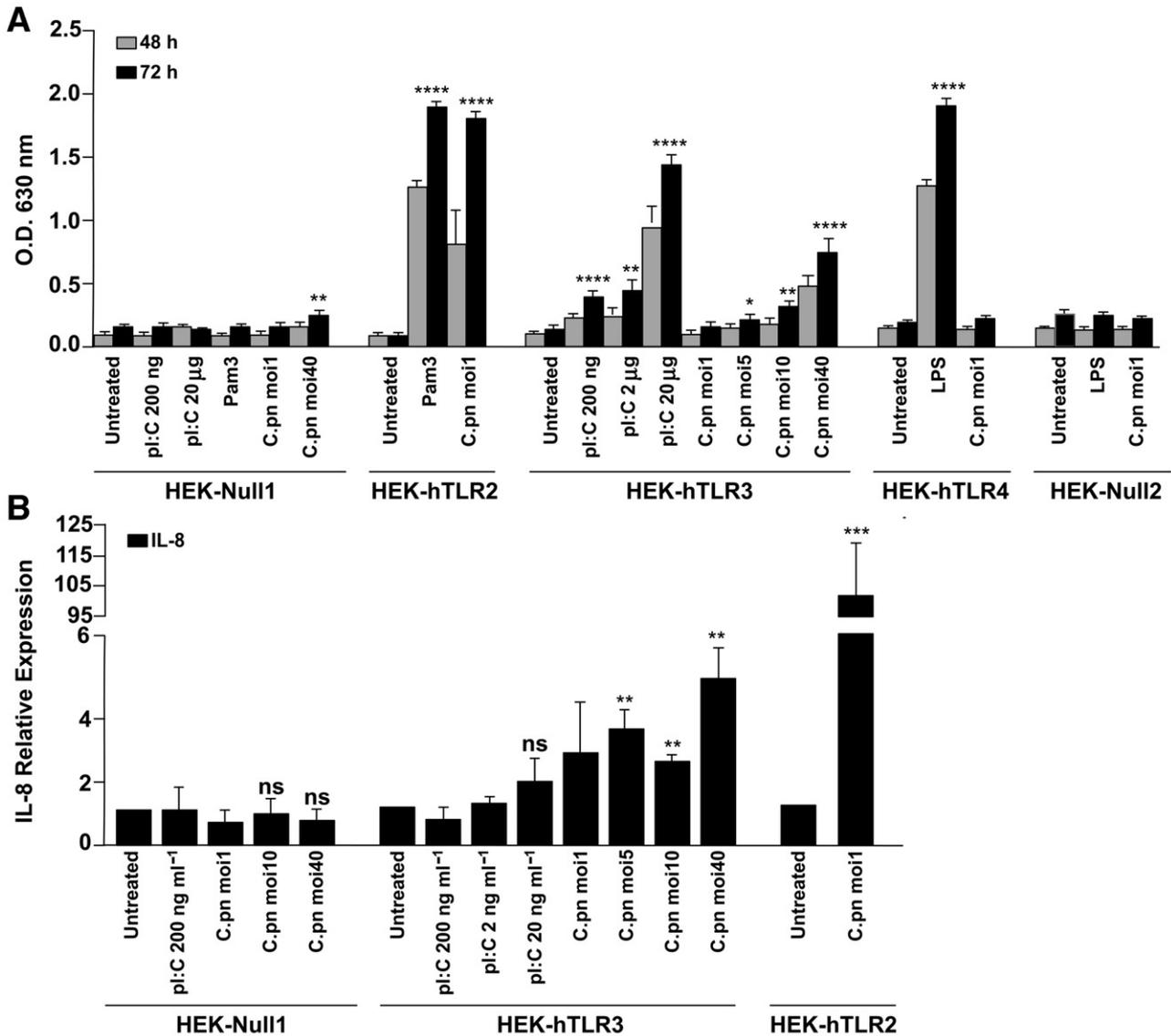
Fig. 7. TLR3 mediates NF-κB activation and IL8 expression.
A. Control HEK cells (HEK-Null) or HEK cells expressing TLR2, TLR3 or TLR4 were infected with *C. pneumoniae* (moi of 1, 5, 10 or 40) or stimulated with the TLR ligands, 5 mg ml^{-1} Pam3CSK4 (TLR2 ligand), 500 ng ml^{-1} LPS (TLR4 ligand) or 200 ng ml^{-1}, 2 mg ml^{-1} or 20 mg ml^{-1} poly(I:C) (TLR3 ligand) for 48 h or 72 h. NF-κB activation was assessed by measuring SEAP activity colorimetrically at 630 nm.
B. HEK cells expressing TLR3 or TLR2 were infected with *C. pneumoniae* at the indicated moi or stimulated with poly(I:C), and IL8 expression was measured by qPCR.
*$P < 0.045$, **$P < 0.01$, ***$P < 0.001$ and ****$P < 0.0005$.

central mediator in regulating inflammation initiated by *C. pneumoniae,* and this complex appears to perform its functions primarily via a potential feedback loop that may interact with TLR3 and MAP3K8. This does not exclude other TF complexes or other signalling pathway components that may be involved in the inflammatory process. In fact, many of the intermediate steps and components in the complex network (Fig. 3) remain to be experimentally discovered. However, we consider our results to be less biased than other biological and experimental conditions because they are drawn from a systems biology-based approach using established and primary cell lines, including experimental validation. Thus, our results are supporting a role for AP-1 in regulating inflammation induced by *C. pneumoniae*. Our findings lay the foundation for further research to expand our understanding of the AP-1 complex and other TF networks in *C. pneumoniae*-stimulated inflammation using appropriate animal models and *in vitro* model systems. In addition, our approach will be important for identifying immunotherapeutic markers as targets for interventions to prevent the inflammatory diseases caused by *C. pneumoniae* such as

atherosclerosis (Campbell and Kuo, 2004) and asthma (Hahn *et al.*, 2012). Indeed, while there are many publications regarding the role of this pathogen in atherosclerosis, the present work may also be important in understanding the pathogenesis of asthma, given the growing body of evidence supporting an association between *C. pneumoniae* and asthma (Metz and Kraft, 2010; Olivares-Zavaleta *et al.*, 2011; Senn *et al.*, 2011; Hahn *et al.*, 2012; Patel *et al.*, 2012).

Experimental procedures

Network assembly

We combined existing network databases and systems network approaches using our previously described methods (Wang *et al.*, 2010). Briefly, our network database included proteins and interactions from BIND (http://bond.unleashedinformatics.com/Action), DIP (http://dip.doe-mbi.ucla.edu/), HPRD (http://hprd.org/), PreBIND (http://www.blueprint.org/system/app/pages/search?scope=search-site&q=PreBIND), curated inflammatory disease databases (Calvano *et al.*, 2005; von Mering *et al.*, 2005; Reiss *et al.*, 2005a,b), biocarta (http://www.biocarta.com/pathfiles/h_inflamPathway.asp, http://www.biocarta.com/pathfiles/h_LairPathway.asp), KEGG (http://www.genome.jp/kegg/pathway.html), EMBL human database (http://www.embl-heidelberg.de/) and two cytokine databases (http://www.siteseostats.net/site/cytokine.medic.kumamoto-u.ac.jp and http://people.bu.edu/gilmore/nf-kb/). This network was then used as a basis for building a *C. pneumoniae* network from whole human genome microarray data of *C. pneumoniae* infection of HCAEC over five experimental time points representing the developmental cycle of the organism (see below).

C. pneumoniae *propagation*

Chlamydia pneumoniae strain A03 (a gift from Dr James Summersgill) was previously isolated from the coronary artery of a patient with atherosclerosis (Ramirez, 1996). This clinical isolate was propagated in HEp-2 cells (ATCC CCL-23; Manassas, VA) following standard laboratory protocols as we have described previously (Ramirez, 1996; Molestina *et al.*, 1998; Mukhopadhyay *et al.*, 2004; Wang *et al.*, 2010). Isolates were purified using 30% RenoCal centrifugation gradients as described (Li *et al.*, 2005; Wang *et al.*, 2010) to eliminate ~ 0.1% of contaminating human cellular material.

HCAEC culture and infection

The cell culture was performed using a previously reported method (Wang *et al.*, 2010). Briefly, Endothelial Cell Basal Medium-2 with hEGF, Hydrocortisone, GA-1000, FBS, VEGF, hFGF-B, R3-IGF-1 and Ascorbic Acid (Clonetics™ EGM®-2-MV BulletKit, East Rutherford, NJ) were used to grow HCAEC (Clonetics™) according to the manufacturer's instructions. The cells were grown in T25 flasks in 37°C with 5% CO_2 to a confluence of ~ 80% and ~ 55%, respectively, for subsequent group 1 (0 min, 5 min, 25 min and 2 h) and group 2 (24 h and 60 h) infections with *C. pneumoniae*. A *C. pneumoniae* moi of 100 and

5 was used for group 1 and group 2 infections respectively. The higher confluence and moi for group 1 was used to ensure sufficient infection for a short period of *C. pneumoniae* growth for RNA extraction. The lower confluence and moi for group 2 allowed the cells to grow and for *C. pneumoniae* to infect these cells for the 24 h and 60 h time points in such a way that neither the cells nor *C. pneumoniae* would overgrow the cell culture system, which could result in apoptosis and loss of infection. For UV inactivation, *C. pneumoniae* was treated with a UV germicidal light for 3 h (30 w, 15 cm). HCAEC were infected as above with UV-treated *C. pneumoniae* at the same moi as for viable *C. pneumoniae*. Mock-infected HCAEC were used as controls for each time point.

RNA extraction, microarray hybridization and array detection

Infected and uninfected HCAEC at 0 min, 5 min, 25 min, 2 h, 24 h and 60 h post infection were trypsinized and collected by centrifugation. RNA was purified using the RNeasy RNA purification kit (QIAGEN, Valencia, CA), including an on column treatment with DNase to eliminate all traces of DNA, according to the manufacturer's instructions and as we have previously described (Gomes *et al.*, 2005). Affymetrix Human Genome U133 Plus 2.0 Arrays, which contain over 47 000 transcripts that completely cover the whole human genome, were employed in this study. GeneChip® One-Cycle Target Labelling and Control Reagents (Affymetrix, Santa Clara, CA) were used to process RNA and for hybridization to the microarrays following the manufacturer's protocols. Briefly, cRNA was generated from total RNA. The resultant biotinylated cRNA was fragmented and hybridized to the microarrays. The arrays were washed, stained and scanned with the Affymetrix scanner using the manufacturer's recommended protocols as per the Stanford University Gene and Protein Expression Core Facility (Palo Alto, CA).

Network analysis

Network analysis was performed as we described in detail previously (Wang *et al.*, 2010). Briefly, genes with significant alterations in gene expression compared with controls in the microarray (*t*-test, $P < 0.05$, as per the Bioconductor package) (Gentleman *et al.*, 2004) were used to overlay the network described above. These overlaid networks became the inflammatory networks activated (up- and downregulated) by *C. pneumoniae*. The activated networks were decomposed into functional modules based on topological interconnection intensity and gene functions (http://www.geneontology.org/) (Bader and Hogue, 2003; Maere *et al.*, 2005; Singhal and Domico, 2007; Singhal and Resat, 2007). Genes were classified according to the gene ontology database (http://www.geneontology.org/) (Garcia *et al.*, 2007).

Standard stepwise regression, which adds and removes variables, was used to select the variables (genes, in our case). The basic method of stepwise regression is to calculate an *F*-statistic for each variable in the model (Hennekens and Buring, 1987). If the *F*-statistic for any variable is less than *F*, the variable with the smallest *F* is removed from the model. If no variable can be removed, the procedure attempts to add a variable. An *F*-statistic is calculated for each variable not yet in the model. The variable

with the largest *F*-statistic is then added, provided its *F*-statistic is larger than *F* to enter. Adding this variable is equivalent to choosing the variable with the largest partial correlation or the variable that most effectively reduces the error sum of squares. The regression equation is then calculated, results are displayed and the procedure continues to a new step. If no variable meets the criteria for addition to the network, the stepwise procedure is finished.

AP-1 binding sites were predicted using the motif Mogul (http://xerad.systemsbiology.net/MotifMogulServer/), with human stringent matrices, stringent MotifLocator Scans at 0.01%, *P* < 0.05, and others as per the default setting in the programs.

Small interfering RNA knock-down

Small interfering RNA (siRNA) knock-down experiments were performed as we previously described (Wang *et al.*, 2010). Briefly, based on the results of the microarray analyses, siRNAs were selected to target AP-1 members, FOS, FOSB, JUN and JUNB (Table S1). To avoid cell line bias, RNAi experiments were also performed in HEp-2 and THP-1 cell lines in addition to HCAEC, which are primary cells. Since results were similar between THP-1 and HCAEC experiments, some experiments were performed with only HEp-2 and THP-1 cell lines owing to the difficulty in working with primary cells.

Cells were cultured to 60%, and siRNAs including scrambled siRNA as a control, were transfected at a 75 nM final concentration, using 0.45% Oligofectamine (Invitrogen, Carlsbad, CA) in a 48-well format. The plates were placed in a tissue culture incubator at 37°C and 5% CO_2. After 48 h of siRNA-mediated gene knock-down, the medium was removed and the cells were infected with *C. pneumoniae* at an moi of 5. After an additional 24 h of incubation as above, each experiment was analysed for quantitative gene expression and protein concentrations as described below. All experiments were performed in triplicate.

Quantitative RT-PCR

Quantitative RT-PCR was performed as we have previously described (Gomes *et al.*, 2005; Wang *et al.*, 2010). Total RNA was extracted using an RNeasy RNA isolation kit (QIAGEN). DNA was digested with RQ DNase (Promega, Madison, WI) at 37°C for 30 min, and cDNA was generated using a Reverse Transcription kit (ABI, Carlsbad, CA). Quantitative real-time reverse transcriptase PCR (qRT-PCR) was run using the Power SYBR Green PCR Kit (ABI) and reagents as we described (Gomes *et al.*, 2005; Wang *et al.*, 2010). The primers for each analyte are shown in Table S2. Each experiment contained negative controls including no template controls, mock-infected HCAEC, HEp-2 or THP-1 cell cDNA and RNA samples without RT. PCR parameters consisted of one cycle of 95°C for 15 min, followed by 40 cycles of PCR at 95°C for 15 s, 55°C for 30 s and 72°C for 30 s. The relative amount of target gene mRNA and 16S bacterial rRNA was normalized to beta-actin mRNA. These experiments were performed in triplicate.

Cytokine protein quantification

Cytokine concentrations for IL2, IL4, IL6, IL8, IL10, IL12, GM-CSF, IFNγ, TNFα and IL1β were tested using Bio-Plex 10-plex kits (Bio-Rad, Hercules, CA) as per the manufacturer's protocols. Briefly, 50 μl of cell culture supernatant for each sample was collected and assayed in duplicate. A range (1.95–32 000 pg ml⁻¹) of standards for each cytokine were resuspended in diluent and used to plot standard curves. Data obtained from Bio-Plex Manager software program (Bio-Rad) for standardization and standard curves were converted to Excel™ (Microsoft Corporation, Seattle, WA) to determine the final concentration for each protein.

NF-κB activity and chemokine expression in HEK-TLR cells

HEK-Blue SEAP reporter cell lines, Null1, Null2, hTLR2, hTLR3 or hTLR4 (Invivogen, San Diego, CA), were grown in T75 flasks with DMEM high glucose media supplemented with 10% FCS, 50 U ml⁻¹ penicillin, 50 mg ml⁻¹ streptomycin and selected with the appropriate antibiotic according to the manufacturer's instructions. Twelve hours prior to stimulation, 1×10^5 HEK-Blue cells per well (24-well plate) were plated. At ~ 50% confluency, cells were left untreated or infected with *C. pneumoniae* at an moi of 1, 5, 10 or 40; or treated with 0.2, 2.0 or 20 mg ml⁻¹ poly I:C (pI:C), 5 mg ml⁻¹ Pam3SCK4 or 0.5 mg ml⁻¹ ultra pure *Escherichia coli* lipopolysaccharide (LPS) as indicated (Invivogen). Supernatants were collected at 48 and 72 hpi for the NF-κB activity assay. Whole cells were collected for RNA isolation (below) at 72 hpi.

Collected supernatants from each sample were mixed at a ratio of 9:1 with QUANTI-Blue solution (Invivogen) in a flat-bottom 96-well plate. The samples were incubated at 37°C for 2 h and then the secretion level of Secreted Embryonic Alkaline Phosphatase (SEAP) was measured at 630 nm using a spectrophotometer.

For measurement of cytokine gene expression by real-time PCR, mRNA was isolated from cells after the indicated treatments using the Qiagen RNeasy kit (QIAGEN) following the manufacturer's instructions. The synthesis of the complementary DNA (cDNA) template was conducted according to the manufacturer's instruction (TaqMan, Roche, Pleasanton, CA). qPCR analysis using Mx3000P (Stratagene, La Jolla, CA) was conducted in triplicates in a 20 ml final volume with Brilliant III Ultra-Fast SYBR Green qPCR master mix (Stratagene). Real-time PCR included initial denaturation at 95°C for 3 min, followed by 40 cycles of 95°C for 5 s, 60°C for 20 s, and one cycle of 95°C for 1 min, 55°C for 30 s, 95°C for 30 s. The average for each treatment was normalized to the activity of a house-keeping gene, GAPDH. The relative expression of IL-8 for each cell type was normalized to the untreated samples. The statistical analysis was carried out using the unpaired *t*-test where **P* < 0.045, ***P* < 0.01, ****P* < 0.001 and *****P* < 0.0005. Data were collected from three independent experiments.

References

Bader, G.D., and Hogue, C.W. (2003) An automated method for finding molecular complexes in large protein interaction networks. *BMC Bioinformatics* **4:** 2.

Balasubramanian, A., Ganju, R.K., and Groopman, J.E. (2003) Hepatitis C virus and HIV envelope proteins collaboratively mediate interleukin-8 secretion through activation of p38 MAP kinase and SHP2 in hepatocytes. *J Biol Chem* **278:** 35755–35766.

Belland, R.J., Ouellette, S.P., Gieffers, J., and Byrne, G.I. (2004) *Chlamydia pneumoniae* and atherosclerosis. *Cell Microbiol* **6:** 117–127.

Betts, H.J., Wolf, K., and Fields, K.A. (2009) Effector protein modulation of host cells: examples in the *Chlamydia* spp. arsenal. *Curr Opin Microbiol* **12:** 81–87.

Botos, I., Liu, L., Wang, Y., Segal, D.M., and Davies, D.R. (2009) The toll-like receptor 3:dsRNA signaling complex. *Biochim Biophys Acta* **1789:** 667–674.

Buchholz, K.R., and Stephens, R.S. (2006) Activation of the host cell proinflammatory interleukin-8 response by *Chlamydia trachomatis. Cell Microbiol* **8:** 1768–1779.

Calvano, S.E., Xiao, W., Richards, D.R., Felciano, R.M., Baker, H.V., Cho, R.J., *et al.* (2005) A network-based analysis of systemic inflammation in humans. *Nature* **437:** 1032–1037.

Campbell, L.A., and Kuo, C.C. (2004) *Chlamydia pneumoniae* – an infectious risk factor for atherosclerosis? *Nat Rev Microbiol* **2:** 23–32.

Cao, F., Castrillo, A., Tontonoz, P., Re, F., and Byrne, G.I. (2007) *Chlamydia pneumoniae*-induced macrophage foam cell formation is mediated by Toll-like receptor 2. *Infect Immun* **75:** 753–759.

Chen, S., Sorrentino, R., Shimada, K., Bulut, Y., Doherty, T.M., Crother, T.R., and Arditi, M. (2008) *Chlamydia pneumoniae*-induced foam cell formation requires MyD88-dependent and -independent signaling and is reciprocally modulated by liver X receptor activation. *J Immunol* **181:** 7186–7193.

Chinenov, Y., and Kerppola, T.K. (2001) Close encounters of many kinds: Fos-Jun interactions that mediate transcription regulatory specificity. *Oncogene* **20:** 2438–2452.

Cho, N.H., Seong, S.Y., Choi, M.S., and Kim, I.S. (2001) Expression of chemokine genes in human dermal microvascular endothelial cell lines infected with *Orientia tsutsugamushi. Infect Immun* **69:** 1265–1272.

Curran, T., and Franza, B.R., Jr (1988) Fos and Jun: the AP-1 connection. *Cell* **55:** 395–397.

Darville, T., O'Neill, J.M., Andrews, C.W., Jr, Nagarajan, U.M., Stahl, L., and Ojcius, D.M. (2003) Toll-like receptor-2, but not Toll-like receptor-4, is essential for development of oviduct pathology in chlamydial genital tract infection. *J Immunol* **171:** 6187–6197.

Dechend, R., Maass, M., Gieffers, J., Dietz, R., Scheidereit, C., Leutz, A., and Gulba, D.C. (1999) *Chlamydia pneumoniae* infection of vascular smooth muscle and endothelial cells activates NF-kappaB and induces tissue factor and PAI-1 expression: a potential link to accelerated arteriosclerosis. *Circulation* **100:** 1369–1373.

Derbigny, W.A., Kerr, M.S., and Johnson, R.M. (2005) Pattern recognition molecules activated by *Chlamydia muridarum* infection of cloned murine oviduct epithelial cell lines. *J Immunol* **175:** 6065–6075.

Derbigny, W.A., Hong, S.C., Kerr, M.S., Temkit, M., and Johnson, R.M. (2007) *Chlamydia muridarum* infection elicits a beta interferon response in murine oviduct epithelial cells dependent on interferon regulatory factor 3 and TRIF. *Infect Immun* **75:** 1280–1290.

Derbigny, W.A., Johnson, R.M., Toomey, K.S., Ofner, S., and Jayarapu, K. (2010) The *Chlamydia muridarum*-induced IFN-beta response is TLR3-dependent in murine oviduct epithelial cells. *J Immunol* **185:** 6689–6697.

Eferl, R., and Wagner, E.F. (2003) AP-1: a double-edged sword in tumorigenesis. *Nat Rev Cancer* **3:** 859–868.

Garcia, M., Jemal, A., Ward, E.M., Center, M.M., Hao, Y., Siegel, R.L., and Thun, M.J. (2007) *Global Cancer Facts & Figures 2007*. Atlanta, GA: American Cancer Society.

Gencay, M.M., Tamm, M., Glanville, A., Perruchoud, A.P., and Roth, M. (2003) *Chlamydia pneumoniae* activates epithelial cell proliferation via NF-kappaB and the glucocorticoid receptor. *Infect Immun* **71:** 5814–5822.

Gentleman, R.C., Carey, V.J., Bates, D.M., Bolstad, B., Dettling, M., Dudoit, S., *et al.* (2004) Bioconductor: open software development for computational biology and bioinformatics. *Genome Biol* **5:** R80.

Gomes, J.P., Hsia, R.C., Mead, S., Borrego, M.J., and Dean, D. (2005) Immunoreactivity and differential developmental expression of known and putative *Chlamydia trachomatis* membrane proteins for biologically variant serovars representing distinct disease groups. *Microbes Infect* **7:** 410–420.

Hahn, D.L., Schure, A., Patel, K., Childs, T., Drizik, E., and Webley, W. (2012) *Chlamydia pneumoniae*-specific IgE is prevalent in asthma and is associated with disease severity. *PLoS ONE* **7:** e35945.

Hennekens, C.H., and Buring, J.E. (1987) Epidemiology in medicine. In *Medicine (Baltimore)*. Mayrent, S.L. (ed.). Boston, MA: Little, Brown and Co., pp. 1–383.

Hogdahl, M., Soderlund, G., and Kihlstrom, E. (2008) Expression of chemokines and adhesion molecules in human coronary artery endothelial cells infected with *Chlamydia* (Chlamydophila) *pneumoniae. APMIS* **116:** 1082–1088.

Huang, B., Dong, Y., Cheng, Y., Xie, Q., Lin, G., Wu, Y., *et al.* (2008) *Chlamydia pneumoniae* infection and hyperlipidaemia-induced expression of P50 and c-Fos in the heart of C57BL6J mice. *Acta Cardiol* **63:** 175–179.

Karin, M., Lawrence, T., and Nizet, V. (2006) Innate immunity gone awry: linking microbial infections to chronic inflammation and cancer. *Cell* **124:** 823–835.

Kaul, R., and Wenman, W.M. (2001) *Chlamydia pneumoniae* facilitates monocyte adhesion to endothelial and smooth muscle cells. *Microb Pathog* **30:** 149–155.

Krull, M., Kramp, J., Petrov, T., Klucken, A.C., Hocke, A.C., Walter, C., *et al.* (2004) Differences in cell activation by *Chlamydophila pneumoniae* and *Chlamydia trachomatis* infection in human endothelial cells. *Infect Immun* **72:** 6615–6621.

Lad, S.P., Li, J., Correia, J., Pan, Q., Gadwal, S., Ulevitch, R.J., and Li, E. (2007) Cleavage of p65/RelA of the NF-kappaB pathway by *Chlamydia. Proc Natl Acad Sci USA* **104:** 2933–2938.

Le Negrate, G., Krieg, A., Faustin, B., Loeffler, M., Godzik, A., Krajewski, S., and Reed, J.C. (2008) ChlaDub1 of *Chlamydia trachomatis* suppresses NF-κB activation and inhibits IκBα ubiquitination and degradation. *Cell Microbiol* **10:** 1879–1892.

Li, D., Vaglenov, A., Kim, T., Wang, C., Gao, D., and Kaltenboeck, B. (2005) High-yield culture and purification of *Chlamydiaceae* bacteria. *J Microbiol Methods* **61:** 17–24.

Maere, S., Heymans, K., and Kuiper, M. (2005) BiNGO: a Cytoscape plugin to assess overrepresentation of gene ontology categories in biological networks. *Bioinformatics* **21:** 3448–3449.

von Mering, C., Jensen, L.J., Snel, B., Hooper, S.D., Krupp, M., Foglierini, M., *et al.* (2005) STRING: known and predicted protein-protein associations, integrated and transferred across organisms. *Nucleic Acids Res* **33:** D433–D437.

Metz, G., and Kraft, M. (2010) Effects of atypical infections with *Mycoplasma* and *Chlamydia* on asthma. *Immunol Allergy Clin North Am* **30:** 575–585.

Miller, S.A., Selzman, C.H., Shames, B.D., Barton, H.A., Johnson, S.M., and Harken, A.H. (2000) *Chlamydia pneumoniae* activates nuclear factor kappaB and activator protein 1 in human vascular smooth muscle and induces cellular proliferation. *J Surg Res* **90:** 76–81.

Misaghi, S., Balsara, Z.R., Catic, A., Spooner, E., Ploegh, H.L., and Starnbach, M.N. (2006) *Chlamydia trachomatis*-derived deubiquitinating enzymes in mammalian cells during infection. *Mol Microbiol* **61:** 142–150.

Molestina, R.E., Dean, D., Miller, R.D., Ramirez, J.A., and Summersgill, J.T. (1998) Characterization of a strain of *Chlamydia pneumoniae* isolated from a coronary atheroma by analysis of the *omp1* gene and biological activity in human endothelial cells. *Infect Immun* **66:** 1370–1376.

Mukhopadhyay, S., Clark, A.P., Sullivan, E.D., Miller, R.D., and Summersgill, J.T. (2004) Detailed protocol for purification of *Chlamydia pneumoniae* elementary bodies. *J Clin Microbiol* **42:** 3288–3290.

Naiki, Y., Michelsen, K.S., Schroder, N.W., Alsabeh, R., Slepenkin, A., Zhang, W., *et al.* (2005) MyD88 is pivotal for the early inflammatory response and subsequent bacterial clearance and survival in a mouse model of *Chlamydia pneumoniae* pneumonia. *J Biol Chem* **280:** 29242–29249.

Nijhara, R., Jana, S.S., Goswami, S.K., Rana, A., Majumdar, S.S., Kumar, V., and Sarkar, D.P. (2001) Sustained activation of mitogen-activated protein kinases and activator protein 1 by the hepatitis B virus X protein in mouse hepatocytes *in vivo*. *J Virol* **75:** 10348–10358.

Olivares-Zavaleta, N., Carmody, A., Messer, R., Whitmire, W.M., and Caldwell, H.D. (2011) *Chlamydia pneumoniae* inhibits activated human T lymphocyte proliferation by the induction of apoptotic and pyroptotic pathways. *J Immunol* **186:** 7120–7126.

Patel, K.K., Anderson, E., Salva, P.S., and Webley, W.C. (2012) The prevalence and identity of *Chlamydia*-specific IgE in children with asthma and other chronic respiratory symptoms. *Respir Res* **13:** 32.

Pikarsky, E., Porat, R.M., Stein, I., Abramovitch, R., Amit, S., Kasem, S., *et al.* (2004) NF-kappaB functions as a tumour promoter in inflammation-associated cancer. *Nature* **431:** 461–466.

Prebeck, S., Kirschning, C., Durr, S., da Costa, C., Donath, B., Brand, K., *et al.* (2001) Predominant role of toll-like receptor 2 versus 4 in *Chlamydia pneumoniae*-induced activation of dendritic cells. *J Immunol* **167:** 3316–3323.

Ramirez, J.A. (1996) Isolation of *Chlamydia pneumoniae* from the coronary artery of a patient with coronary atherosclerosis. The *Chlamydia pneumoniae*/Atherosclerosis Study Group. *Ann Intern Med* **125:** 979–982.

Ravichandran, V., Sabath, B.F., Jensen, P.N., Houff, S.A., and Major, E.O. (2006) Interactions between c-Jun, nuclear factor 1, and JC virus promoter sequences: implications for viral tropism. *J Virol* **80:** 10506–10513.

Reiss, D.J., Avila-Campillo, I., Thorsson, V., Schwikowski, B., and Galitski, T. (2005a) Tools enabling the elucidation of molecular pathways active in human disease: application to Hepatitis C virus infection. *BMC Bioinformatics* **6:** 154.

Reiss, K., Maretzky, T., Ludwig, A., Tousseyn, T., de Strooper, B., Hartmann, D., and Saftig, P. (2005b) ADAM10 cleavage of N-cadherin and regulation of cell–cell adhesion and beta-catenin nuclear signalling. *EMBO J* **24:** 742–752.

Selzman, C.H., Netea, M.G., Zimmerman, M.A., Weinberg, A., Reznikov, L.L., Grover, F.L., and Dinarello, C.A. (2003) Atherogenic effects of *Chlamydia pneumoniae*: refuting the innocent bystander hypothesis. *J Thorac Cardiovasc Surg* **126:** 688–693.

Senn, L., Jaton, K., Fitting, J.W., and Greub, G. (2011) Does respiratory infection due to *Chlamydia pneumoniae* still exist? *Clin Infect Dis* **53:** 847–848.

Seo, J.H., Lim, J.W., Kim, H., and Kim, K.H. (2004) *Helicobacter pylori* in a Korean isolate activates mitogen-activated protein kinases, AP-1, and NF-kappaB and induces chemokine expression in gastric epithelial AGS cells. *Lab Invest* **84:** 49–62.

Sessa, R., Di Pietro, M., Schiavoni, G., Macone, A., Maras, B., Fontana, M., *et al.* (2009) *Chlamydia pneumoniae* induces T cell apoptosis through glutathione redox imbalance and secretion of TNF-alpha. *Int J Immunopathol Pharmacol* **22:** 659–668.

Shaulian, E., and Karin, M. (2002) AP-1 as a regulator of cell life and death. *Nat Cell Biol* **4:** E131–E136.

Singhal, M., and Domico, K. (2007) CABIN: collective analysis of biological interaction networks. *Comput Biol Chem* **31:** 222–225.

Singhal, M., and Resat, H. (2007) A domain-based approach to predict protein–protein interactions. *BMC Bioinformatics* **8:** 199.

Takeuchi, O., and Akira, S. (2009) Innate immunity to virus infection. *Immunol Rev* **227:** 75–86.

Vallejo, J.G., Knuefermann, P., Mann, D.L., and Sivasubramanian, N. (2000) Group B Streptococcus induces TNF-alpha gene expression and activation of the transcription factors NF-kappa B and activator protein-1 in human cord blood monocytes. *J Immunol* **165:** 419–425.

Vercammen, E., Staal, J., and Beyaert, R. (2008) Sensing of viral infection and activation of innate immunity by toll-like receptor 3. *Clin Microbiol Rev* **21:** 13–25.

Wang, A., Johnston, S.C., Chou, J., and Dean, D. (2010) A systemic network for *Chlamydia pneumoniae* entry into human cells. *J Bacteriol* **192:** 2809–2815.

Wolf, K., Plano, G.V., and Fields, K.A. (2009) A protein

secreted by the respiratory pathogen *Chlamydia pneumoniae* impairs IL-17 signaling via interaction with human Act1. *Cell Microbiol* **11:** 769–779.

Wu, J.Y., Lu, H., Sun, Y., Graham, D.Y., Cheung, H.S., and Yamaoka, Y. (2006) Balance between polyoma enhancing activator 3 and activator protein 1 regulates *Helicobacter pylori*-stimulated matrix metalloproteinase 1 expression. *Cancer Res* **66:** 5111–5120.

Xie, J., Pan, H., Yoo, S., and Gao, S.J. (2005) Kaposi's sarcoma-associated herpesvirus induction of AP-1 and interleukin 6 during primary infection mediated by multiple mitogen-activated protein kinase pathways. *J Virol* **79:** 15027–15037.

Ye, F.C., Blackbourn, D.J., Mengel, M., Xie, J.P., Qian, L.W., Greene, W., *et al*. (2007) Kaposi's sarcoma-associated herpesvirus promotes angiogenesis by inducing angiopoietin-2 expression via AP-1 and Ets1. *J Virol* **81:** 3980–3991.

Yeo, M., Park, H.K., Lee, K.M., Lee, K.J., Kim, J.H., Cho, S.W., and Hahm, K.B. (2004) Blockage of HSP 90 modulates Helicobacter pylori-induced IL-8 productions through the inactivation of transcriptional factors of AP-1 and NF-kappaB. *Biochem Biophys Res Commun* **320:** 816–824.

Yu, H., Kim, P.M., Sprecher, E., Trifonov, V., and Gerstein, M. (2007) The importance of bottlenecks in protein networks: correlation with gene essentiality and expression dynamics. *PLOS Comput Biol* **3:** e59.

Zachos, G., Clements, B., and Conner, J. (1999) Herpes simplex virus type 1 infection stimulates p38/c-Jun N-terminal mitogen-activated protein kinase pathways and activates transcription factor AP-1. *J Biol Chem* **274:** 5097–5103.

Supporting information

Additional Supporting Information may be found in the online version of this article:

Table S1. Gene and nucleotide sequences of small interfering RNA.
Table S2. Primers used for quantitative real-time PCR.

Supporting Information

Transcription Factor Complex AP-1 Mediates Inflammation Initiated by *Chlamydia pneumoniae* Infection

Anyou Wang, Mufadhal Al-Kuhlani, S. Clayborne Johnston, David M. Ojcius, Joyce Chou, Deborah Dean

Supplementary Table S1. Gene and nucleotide sequences of small interfering RNA

Supplementary Table S2. Primers used for quantitative real time PCR.

Supplementary Table S1. Gene and nucleotide sequences of small interfering RNA.

Accession	Position	Locus	Sequence
FOS	14q24.3	2353	5' – CACUCCAAGCGGAGACAGATT –3' 5' – UCUGUCUCCGCUUGGAGUGTA –3' 5' – CUUCCUUCGUCUUCACCUATT –3' 5' – UAGGUGAAGACGAAGGAAGAC –3'
JUN	1p32-p31	3725	5' – GGCACAGCUUAAACAGAAATT –3' 5' – UUUCUGUUUAAGCUGUGCCAC –3' 5' – CCAAGUGCCGAAAAAGGAATT –3' 5' – UUCCUUUUUCGGCACUUGGAG –3'
	19p13.2	3726	5' – CUCUCUACACGACUACAAATT –3' 5' – UUUGUAGUCGUGUAGAGAGAG –3' 5' – GCCUCUCUCUACACGACUATT –3' 5' – UAGUCGUGUAGAGAGAGGCCA –3'
	19q13.32	2354	5' – CCGGGAACGAAAUAAACUATT –3' 5' – UAGUUUAUUUCGUUCCCGGCG –3' 5' – ACUUCUUCGUUUGUCCUCATT –3' 5' – UGAGGACAAACGAAGAAGUGT –3'
Scrambled			5' – UAAGGCUAUGAAGAGAUACdTdT –3' 5' – dTdTAUUCCGAUACUUCUCUAUGA –3'

Supplementary Table S2. Primers used for quantitative real time PCR.

Gene Name	Sequence
FOS	5' – CCGCTTGGGAGTGTATCAGTCA – 3'
FOS-1	5' – GGGCAAGGTGGAACAGTTATC – 3'
JUN	5' – GGCGATTCTCTCCAGCTTCC – 3'
JUN-1-1	5' – TCGACATGGAGTCCCAGGA – 3'
TNF	5' – GCTACAGGCTTGTCACTCGG – 3'
TNF-1	5' – CCCAGGGACCTCTCTCTAATCA – 3'
IL6	5' – GCATTTGCTCTCTGCTAAGTTCC – 3'
IL6-1	5' – CTGTATCACAGACTGGCAACAAG – 3'
IL8	5' – ACTACTGTAATCCTAACACCTG – 3'
IL8-1	5' – ATTGAGAGTGGACCACACTG – 3'
CD38	5' – GCAAGGTACGGTCTGAGTTCC – 3'
CD38-1	5' – AGACTGCCAAAGTGTATGGGA – 3'
TLR3	5' – CAAACACAAGCATTCGGAATCTG – 3'
TLR3-1	5' – AAGAAAGTTGTATTGCTGGTGGT – 3'
MAP3K8	5' – TGGCTCTTCACTTGCATAAAGAT – 3'
MAP3K8-1	5' – ATGGAGTACATGAGCACTGGA – 3'
JUNB	5' – CGCTTTGAGACTCCGGTAGG – 3'
JUNB-1	5' – TACCACGACGACTCATACACA – 3'
FOSB	5' – GCACCCTTCGCTTCTCCTC – 3'
FOSB-1	5' – ACCAGCTACTCCACACCAG – 3'
ICAM1F	5' – TCTGTGTCCCCCTCAAAAGTC – 3'
ICAM1R	5' – GGGGTCTCTATGCCCAACAA – 3'
TANKF	5' – CCATCCATCACATCTGTCACAC – 3'
TANKR	5' – AGTCATTGTCCATAGGTGGAAAC – 3'
CARD15F	5' – GAAAGAGCAAGTGTCCTCCTC – 3'
CARD15R	5' – CTCCTCTGTGCCTGAAAAGC – 3'
RNASELF	5' – TTGAGGCGAAAGACAAAGGAG – 3'
RNASELR	5' – GTCACAGGCGTTTACATCTGC – 3'
DDX58F	5' – TGTGCTCCTACAGGTTGTGGA – 3'
DDX58R	5' – CACTGGGATCTGATTCGCAAAA – 3'
IFIH1F	5' – CAACATGGGCAGTGATTCAGG – 3'
IFIH1R	5' – TGGGCAACTTCCATTTGGTAAG – 3'
SPG7F	5' – CCTGTGGTATGTTTTCCGTCTG – 3'
SPG7R	5' – AGTTTGGCTTCGTGCATTCCT – 3'
MYD88F	5' – GCTGAGAAGCCTTTACAGGTG – 3'
MYD88R	5' – CTGGGGCAATAGCAGATGAAG – 3'
IRF1F	5' – CTTCCACCTCTCACCAAGAAC – 3'
IRF1R	5' – CCATCAGAGAAGGTATCAGGGC – 3'
IRF2F	5' – ATGCGGCTAGACATGGGTG – 3'
IRF2R	5' – GCATCTGAAATTCGCCTTCCA – 3'
IRF7F	5' – GCTGGACGTGACCATCATGTA – 3'
IRF7R	5' – GGGCCGTATAGGAACGTGC – 3'

IRF3F	5' – GTGGCCTGGGTGAACAAGAG – 3'
IRF3R	5' – CTGGAAGATTCCGAAATCCTCC – 3'
IRF6F	5' – CTGCGCTGTGCTCTCAATAAG – 3'
IRF6R	5' – TCCTGGGTTAATGATCGAGCC – 3'
IFNB1F	5' – ATGACCAACAAGTGTCTCCTCC – 3'
IFNB1R	5' – GCTCATGGAAAGAGCTGTAGTG – 3'
MX1F	5' – TTCCGAAGTGGACATCGCAAA – 3'
MX1R	5' – ACCGAGCCTGGATTTTTCTGG – 3'
MX2F	5' – CAGCAGACGATCAACTTGGTG – 3'
MX2R	5' – CATGACGCTTTTCTCAGTGCC – 3'
PTGS2F	5' – ATATGTTCTCCTGCCTACTGGAA – 3'
PTGS2R	5' – GCCCTTCACGTTATTGCAGATG – 3'
NFKBIAF	5' – CTCCGAGACTTTCGAGGAAATAC – 3'
NFKBIAR	5' – GCCATTGTAGTTGGTAGCCTTCA – 3'